On nanoscale metallic iron for groundwater remediation

Noubactep C.*[(a,c)] , Caré S.[(b)]

[(a)] Angewandte Geologie, Universität Göttingen, Goldschmidtstraße 3, D - 37077 Göttingen, Germany;

[(b)] Université Paris-Est, Laboratoire Navier, Ecole des Ponts - ParisTech, LCPC, CNRS, 2 allée Kepler, 77420 Champs sur Marne, France;

[(c)] Kultur und Nachhaltige Entwicklung CDD e.V., Postfach 1502, D - 37005 Göttingen, Germany.

* corresponding author: e-mail: cnoubac@gwdg.de; Tel. +49 551 39 3191, Fax: +49 551 399379

(Accepted 02.06.2010)

Abstract

This communication challenges the concept that nanoscale metallic iron (nano-Fe^0) is a strong reducing agents for contaminant reductive transformation. It is shown that the inherent relationship between contaminant removal and Fe^0 oxidative dissolution which is conventionally attributed to contaminant reduction by nano-Fe^0 (direct reduction) could equally be attributed to contaminant removal by adsorption and co-precipitation. For reducible contaminants, indirect reduction by adsorbed Fe^{II} or adsorbed H produced by corroding iron (indirect reduction) is even a more probable reaction path. As a result, the contaminant removal efficiency is strongly dependent on the extent of iron corrosion which is larger for nano-Fe^0 than for micro-Fe^0 in the short term. However, because of the increased reactivity, nano-Fe^0 will deplete in the short term. No more source of reducing agents (Fe^{II}, H, H_2) will be available in the system. Therefore, the efficiency of nano-Fe^0 as a reducing agent for environmental remediation is yet to be demonstrated.

Keywords: Adsorption; Co-precipitation, Nanoscale iron; Reduction; Zerovalent iron.

Capsule: The scientific basis for the observed efficiency of nanoscale metallic iron for environmental remediation is yet to be systematically addressed.

1 Introduction

Increased soil and groundwater contamination has prompted researchers to investigate affordable and efficient strategies for environmental protection. One recent innovative possibility has been the use of microscale granular metallic iron (micro-Fe^0 or Fe^0), initially for reductive dechlorination of halogenated carbons [1-4]. The success of Fe^0 for reductive dechlorination has encouraged researchers to test its applicability to several other classes of substances [4-10]. In the meantime Fe^0 is considered as a universal material for unspecific contaminant removal from aqueous systems [6,8,11,12]. It is essential to note that neither isolated Fe^0 nor its individual corrosion products are responsible for quantitative contaminant removal. The whole dynamic process of Fe^0 oxidative dissolution coupled to iron hydroxide precipitation and crystallization at pH > 4.5 is responsible of contaminant removal and sequestration [12,13]. In this dynamic process, contaminant reduction via surface-mediated reaction (by Fe^0, adsorbed Fe^{II} or adsorbed H) is likely to occur but the discussion of its extent is a complex issue. It is the intension of this communication to draw the attention of the scientific community on this key issue for nanoscale Fe^0 injected into the subsurface for groundwater remediation.

2. Nanoscale iron for groundwater remediation

Reducing the particle size of granular Fe^0 materials (mm) to 10–100 nm (nanoscale Fe^0 or nano-Fe^0) increases surface area and thus chemical reactivity. Potentially, nano-Fe^0 can be readily placed in the subsurface in slurry form via injection to contaminated zones located well below the ground surface [14,15]. The creation of reactive zones by nano-Fe^0 injection, e.g. via monitoring wells extents the applicability of Fe^0 technology to depths for which engineered Fe^0 walls may be prohibitively expensive [15]. Currently nano-Fe^0 is mostly synthesized via the borohydride-catalyzed reduction of dissolved Fe^{II} or Fe^{III} [16-18]. The reactivity of nano-Fe^0 is sometimes further enhanced by plating Fe^0 by more electropositive metals (e.g. Pd, Ni) to form so-called nanoscale bimetallic particles [19].

An inherent problem of nanoscale particles in aqueous solutions is the formation of aggregates (particle aggregation). The aggregation of single nanoscale particles to micrometer size aggregates is coupled with reduced availability and transport limitations [20-23]. Accordingly, nano-Fe^0 must be readily dispersible in water such that they can migrate through water saturated porous media to the domain where the reactive zone is to be built. Clearly, for in situ environmental remediation, colloidal stability of aqueous nano-Fe^0 dispersions is a critical property [24,25]. To enhance nano-Fe^0 colloidal stability several tools have been developed in recent years [23-25]. For example, Phenrat et al. [24] could stabilize nano-Fe^0 dispersions against aggregation and sedimentation by adsorbing anionic polyelectrolytes on their surface. Using a support material for nano-Fe^0 is another way to solve the aggregation problem. Due to their inexpensiveness, availability, environmental stability, abundant natural resources (e.g. clay minerals, zeolites) are suitable candidates to work as supporting materials [23,26]. As an example, Frost et al. [23] reported increased methylene blue discoloration by a natural palygorskite impregnated with Fe^0.

3. Rationale for enhanced reactivity of nano-Fe^0

Increased nano-Fe^0 efficiency for contaminant removal relative to granular Fe^0 can be mathematically demonstrated on the basis of the ratio surface to diameter of the particles. The relation between the specific surface area (SSA) of a spherical particle and its diameter is given by Eq. 1 [15]

$$SSA = 6/\rho*d \quad (1)$$

Where d is the diameter of the spherical Fe^0 particle and ρ = 7,800 kg/m^3 the specific weight of iron. Eq. 1 shows that the smaller the particle size (d), the larger the specific surface area (SSA). For example, a granular Fe^0 having a mean diameter of 50 μm theoretically has a SSA of about 15 m^2/kg while a nano-Fe^0 with a mean particle diameter of 50 nm has a SSA of about 15,000 m^2/kg. That is a reactivity ratio of 1,000 (10^3). This large reactivity ratio explains why nano-Fe^0 is much more reactive than granular Fe^0. Actually, what is the

meaning of "more reactive"? The next section will attempt to answer this question while considering that the same material is available in micro and nano-size.

4. Significance of increased reactivity of nano-Fe^0

4.1. Modeling iron dissolution

Assuming the same material, available in two fractions: micro-Fe^0 (material 1, d_1 = 50 μm) and nano-Fe^0 (material 2, d_2 = 50 nm), the material reactivity is solely a function of the particle size. If parallel experiments are performed with 0.25 g ($2.5*10^{-4}$ kg or 250 mg) of each material, the number of Fe^0 particles at the beginning of the experiment can be calculated using Eq. 2:

$$N = \frac{M}{\rho_{Fe}.4/3\pi.R_0^3} \quad (2)$$

where M is the mass of Fe^0 ($2.5*10^{-4}$ kg), ρ_{Fe} is the specific weight of Fe (7,800 kg/m^3) and R_0 is the initial radius of the Fe particle (R_1 = 25 μm or R_2 = 25 nm).

Calculations (table 1) show that N_1 = 1958042 and N_2 = $1{,}96.10^{15}$ particles are equivalent to $2.5*10^{-4}$ kg of Fe^0. The corresponding ratio N_2/N_1 (= 10^9 = $[(10^3)^3]$) gives a more realistic explanation of the reactivity difference than the ratio of SSA (10^3). The number of Fe^0 atoms per particle (N') and the number of Fe^0 atoms at the surface of each particle (N'') are evaluated in both cases. Calculations are made by considering the following formula (Eq. 3 and Eq. 4) for the spheres:

$$V = 4/3(\pi R^3) \quad (3)$$

$$S = 4\pi R^2 \quad (4)$$

Fe (α-Fe) is body-centered cubic (bcc) in structure. The bcc system has one atom in the center of the unit cell in addition to the eight corner atoms. It thus has a net total of two atoms per unit cell (2 Fe per cube). The lattice parameter of α-Fe is a = 2.866 Å (1 Å = 10^{-10} m). The corresponding volume is given by $V = a^3$ and the cross section by $S = a^2$. A monolayer is supposed to be made up of individual unit cells of Fe^0 (cubes). Accordingly, each layer has a

thickness of a (lattice parameter) and its cross section S is the area occupied by 2 Fe^0. Calculations attested that there are 10^9 times more Fe^0 in and at the surface of micro Fe^0 than in nano Fe^0 (table 1).

4.2 Discussion of modeling results

Assuming uniform corrosion for spherical particles, the corrosion process of concentric layers of Fe^0 yields concentric layers of iron oxides (iron corrosion products) (Fig. 1). The number of Fe atom per particle can be calculated using Eq. 5.

$$N' = 2.[4/3(\pi R^3)]/a^3 \quad (5)$$

Similarly, the number of Fe atom at the surface of each particle can be calculated using Eq. 6.

$$N'' = 2.[4\pi R^2]/a^2 \quad (6)$$

The factor "2" in Eq. 5 and Eq. 6 accounts for the fact that each unit cell contains 2 Fe atoms. Calculations shown that $9.36*10^{16}$ atoms ($1.55*10^{-7}$ moles or 0.155 μmol) of Fe^0 is dissolved in the first stage of micro-Fe^0 corrosion versus $9.36*10^{19}$ atoms ($1.55*10^{-4}$ moles or 155 μmol) for nano-Fe^0. This corresponds to a molar ratio of 10^3 and is the most elegant way to explain increased reactivity of nano-Fe^0 relative to micro-Fe^0. The reactivity ratio based on the specific surface area was also 10^3 and that based on the number of particles 10^9. Although all three approaches exhibit the same trend, Fe^0 oxidative dissolution is a chemical process which is discussed the best on the basis of molar ratios (from the surface). Additionally, the amount of available contaminant has to be considered as well. In other words the molar ratio of dissolved Fe to available contaminants should be used to discuss difference in reactivity.

For example, complete dissolution of 250 mg Fe^0 yields 4.47 mM Fe^{II}. Nano-Fe^0 (88 layers per particle) is depleted when only 0.3 % of micro-Fe^0 is dissolved (see also Fig 2). Assuming that the initial contaminant concentration is 84 μM (e.g. 20 mg/L uranium), the molar ratio Fe^{II}/contaminant is larger than 53 in the nano-Fe^0 system at Fe^0 depletion. In the system with the micro-iron (0.3 % consumption at 88 layers), the molar ratio Fe^{II}/contaminant is only 0.16. Actually, the dissolution of the first layer of nano-Fe^0 yields 152 μM Fe^{II} which corresponds

to 1.8 times the stoichiometric amount of Fe^0 necessary for the reduction of the contaminant (84 μM). On the other hand, to reduce the 84 μM of contaminant 552 layers of the micro-Fe^0 should be dissolved. All this calculations have intentionally neglected (i) Fe^0 oxidation by water, (ii) precipitation of Fe^{II}/Fe^{III} species, (iii) contaminant reduction by Fe^{II} or H/H_2, and (iv) the differential dissolution kinetics of particle of different sizes. Nevertheless, it is clear that the current approach of comparing Fe^0 material of different size should be improved.

The relevance of such pre-experimental theoretical calculations for future works is depicted in table 2. Tab. 2 compares some important issues of the experimental conditions of Katsenovich and Miralles-Wilhelm [27] and three of the references therein. The four works obviously employed varying experimental procedures to characterize the efficiency of nano-Fe^0 for 12 different compounds. These procedures differ in initial contaminant concentration, Fe^0 dosage, Fe^0 preparation, particle size (10 - 200 nm), volume of experimental bottles, volume of added solution (50 - 150 mL), experimental time, mixing type and mixing intensities. The lack of systematic study designed to elucidate the effects of operational conditions on the efficiency of nano-Fe^0 has certainly complicated the elucidation of the intrinsic reactivity of these materials.

5 Mechanism of contaminant removal by nano-Fe^0

The hart fact that nano-Fe^0 is more reactive and extremely efficient for contaminant removal compared to granular Fe^0 (mm and μm) is certainly due to their increased surface area as confirmed above by calculations. However, this evidence tells little about the real mechanism of contaminant removal. In fact, increased Fe^0 reactivity also means increased iron corrosion product generation. From these corrosion products Fe^{II} (dissolved or adsorbed) and hydrogen (atomic or molecular) are also reducing agents and should be regarded as co-reductants rather that iron corrosion products (ICPs). These co-reductants do compete with non-corroded Fe^0 for contaminant reductive transformation. On the other hand, precipitated and precipitating ICPs are contaminant scavengers. Contaminants enmeshed in the structure of precipitating

ICPs could be further reduced by co-reductants as demonstrated for micro-scale Fe^0 [6,8]. In other words, it is not likely, that increased reactivity changes the fundamental mechanism of contaminant removal by Fe^0. This statement is supported by a recent report from Nawrocki et al. [31] showing that "steady water" has reductive properties in a Fe^0-based water pipe. The reductive characteristic of corrosion scales on iron is well-documented [6,32]. The so-called "steady water" is an electrolyte and can dissolve reducing agents and facilitate the transport of reactive species. As discussed above for 250 mg of Fe^0, Fe^0 depletion occurs in the nano-Fe^0 system as only 0.3 % is consumed in the micro-Fe^0 system (Fig. 2). In groundwater, anoxic conditions prevail and iron oxidation is coupled with water electrolysis resulting in the production of hydrogen (molecular and atomic). Adsorbed Fe^{II}, dissolved Fe^{II}, atomic (H) and molecular (H_2) hydrogen all served as an electron donor for contaminant reduction. Therefore, the reported high-effective reduction by nano-Fe^0 results from reducing conditions created by providing the system in the short-term with elevated amount of electron donors. Accordingly, contaminant reduction induced by nano-Fe^0 is efficient for the short term. The question is how long these reductive conditions will prevail or whether they could manage to reductively transformed the whole contamination.

6 Efficiency of nano-Fe^0 reactive zones

The first problem of reactive zones is inherent to the high reactivity of nano-Fe^0 [33]. Unlike inert adsorbents (e.g. activated carbons) having an adsorbing area (adsorption capacity) which is only "reserved" to contaminants, nano-Fe^0 are readily oxidized by water and the primary products (Fe^{II}, H/H_2) are transported by water or are adsorbed on Fe^0, solid corrosion products or geo-materials. Unless nano-Fe^0, is added to sustain a process in the subsurface its efficiency in the short and middle term is questionable. In fact, whether nano-Fe^0 is transported to the reactive zone or not, it will be oxidized by water. Nano-Fe^0 oxidation can be accelerated by contaminants which are then reduced more likely by co-reductants [6,8]. But once Fe^0 is depleted, no subsequent supply of co-reductants is possible. From this time

on, quantitative contaminant removal can only be attributed to adsorption on iron corrosion products and available biomaterials. The long-term stability of adsorbed contaminants is uncertain. On the other hand, the long-term stability of contaminant removal in micro-Fe^0 systems is mainly due to their continuous enmeshment in the matrix of in-situ generated corrosion products in the inter-particular space (pores) within the Fe^0 wall [12]. Beside the side exclusion favouring this dynamic process, the long-term availability of Fe^0 was the other warrant for this mechanism. The efficiency of size exclusion in reactive zone is uncertain and Fe^0 depletion is rapid. Therefore, the stability of removed contaminants in reactive zone created by nano-Fe^0 injection is uncertain.

7 Concluding remarks

This communication has complained that the reaction kinetics in systems with nano-Fe^0 is not properly considered in the current discussion of the efficiency of reactive zones. More reactive materials (smaller particle size) may rapidly reduced contaminants but also rapidly produced co-reductants. Accordingly, it is still not certain whether the Fe^0 surface (direct reduction) plays any important role in the process of contaminant removal in Fe^0/H_2O systems. Fortunately, for micro-Fe^0 removed contaminants are enmeshed in the matrix of iron corrosion products and are stable under natural conditions [34]. For nano-Fe^0 however, upon Fe^0 depletion contaminants will be simply adsorbed on aged iron corrosion products. In other words, although nano-Fe^0 is currently regarded as an established remediation technology, its efficiency is still to be demonstrated.

Acknowledgments

Sven Hellbach (student research assistant) is acknowledged for technical assistance. The manuscript was improved by the insightful comments of anonymous reviewers from Journal of Hazardous Materials.

References

205 [1] R.W. Gillham, S.F O'Hannesin, Enhanced degradation of halogenated aliphatics by zero-
206 valent iron, Ground Water 32 (1994), 958–967.
207 [2] L.J. Matheson, P.G. Tratnyek, Reductive dehalogenation of chlorinated methanes by iron
208 metal, Environ. Sci. Technol. 28 (1994), 2045–2053.
209 [3] S.F. O´Hannesin, R.W. Gillham, Long-term performance of an in situ "iron wall" for
210 remediation of VOCs, Ground Water 36 (1998), 164–170.
211 [4] M.M. Scherer, S. Richter, R.L. Valentine, P.J.J. Alvarez, Chemistry and microbiology of
212 permeable reactive barriers for in situ groundwater clean up, Rev. Environ. Sci.
213 Technol. 30 (2000), 363–411.
214 [5] A.D. Henderson, A.H. Demond, Long-term performance of zero-valent iron permeable
215 reactive barriers: a critical review, Environ. Eng. Sci. 24 (2007), 401–423.
216 [6] C. Noubactep, Processes of contaminant removal in "Fe^0–H_2O" systems revisited, The
217 importance of co-precipitation. Open Environ. J. 1 (2007), 9–13.
218 [7] A.B. Cundy, L. Hopkinson, R.L.D. Whitby, Use of iron-based technologies in
219 contaminated land and groundwater remediation: A review, Sci. Tot. Environ. 400
220 (2008), 42–51.
221 [8] C. Noubactep, A critical review on the mechanism of contaminant removal in Fe^0–H_2O
222 systems, Environ. Technol. 29 (2008), 909–920.
223 [9] M. Diao, M. Yao, Use of zero-valent iron nanoparticles in inactivating microbes, Water
224 Res. 43 (2009), 5243–5251.
225 [10] T. Pradeep, Anshup, Noble metal nanoparticles for water purification: A critical review,
226 Thin Solid Films 517 (2009), 6441–6478.
227 [11] C. Noubactep, A. Schöner, P. Woafo, Metallic iron filters for universal access to safe
228 drinking water, Clean 37 (2009), 930–937.
229 [12] C. Noubactep, The suitability of metallic iron for environmental remediation, Environ.
230 Progr. (2009) doi: 10.1002/ep.10406.

[13] C. Noubactep, A. Schöner, M. Sauter, Significance of oxide-film in discussing the mechanism of contaminant removal by elemental iron materials, In "Photo-Electrochemistry & Photo-Biology for the Sustainablity"; S. Kaneco, B. Viswanathan, H. Katsumata (Eds.), Bentham Science Publishers 1 (2010), 34–55.

[14] C.B. Wang, W.-X. Zhang, Synthesizing nanoscale iron particles for rapid and complete dechlorination of TCE and PCBs, Environ. Sci. Technol. 31 (1997), 2154–2156.

[15] C. Macé, S. Desrocher, F. Gheorghiu, A. Kane, M. Pupeza, M. Cernik, P. Kvapil, R. Venkatakrishnan, W.-X. Zhang, Nanotechnology and groundwater remediation: A step forward in technology understanding, Remediation 16 (2006), 23–33.

[16] W-x. Zhang, Nanoscale iron particles for environmental remediation: an overview, J. Nanopart. Res. 5 (2003), 323–32.

[17] Z. Xiong, D. Dongye Zhao, G. Pan, Rapid and controlled transformation of nitrate in water and brine by stabilized iron nanoparticles, J. Nanopart. Res. 11 (2009), 807–819.

[18] J.T. Olegario, N. Yee, M. Miller, J. Sczepaniak, B. Manning, Reduction of Se(VI) to Se(-II) by zerovalent iron nanoparticle suspensions, J. Nanopart. Res. (2009), doi: 10.1007/s11051-009-9764-1.

[19] W.-x. Zhang, C.-B. Wang, H.-L. Lien, Treatment of chlorinated organic contaminants with nanoscale bimetallic particles, Catal Today 40 (1998), 387–95.

[20] T. Phenrat, N. Saleh, K. Sirk, R.D. Tilton, G.V. Lowry, Aggregation and sedimentation of aqueous nanoscale zerovalent iron dispersions, Environ. Sci. Technol. 41 (2007), 284–290.

[21] M. Baalousha, Aggregation and disaggregation of iron oxide nanoparticles: Influence of particle concentration, pH and natural organic matter, Sci. Tot. Environ. 407 (2009), 2093–2101.

255 [22] B. Gilbert, R.K. Ono, K.A. Ching, C.S. Kim, The effects of nanoparticle aggregation
256 processes on aggregate structure and metal uptake, J. Colloid Interf. Sci. 339 (2009),
257 285–295.
258 [23] R.L. Frost, Y. Xi, H. He, Synthesis, characterization of palygorskite supported zero-
259 valent iron and its application for methylene blue adsorption, J. Colloid Interf. Sci. 341
260 (2010), 153–161.
261 [24] T. Phenrat, N. Saleh, K. Sirk, H.-J. Kim, R.D. Tilton, G.V. Lowry, Stabilization of
262 aqueous nanoscale zerovalent iron dispersions by anionic polyelectrolytes: adsorbed
263 anionic polyelectrolyte layer properties and their effect on aggregation and
264 sedimentation, J. Nanopart. Res. 10 (2008), 795–814.
265 [25] H. Kim, H.-J. Hong, J. Jung, S.-H. Kim, J.-W. Yang, Degradation of trichloroethylene
266 (TCE) by nanoscale zero-valent iron (nZVI) immobilized in alginate bead, J. Hazard.
267 Mater. 176 (2010), 1038–1043.
268 [26] J.R. Kiser, B.A. Manning, Reduction and immobilization of chromium(VI) by iron(II)-
269 treated faujasite, J. Hazard. Mater. 174 (2010), 167–174.
270 [27] Y.P. Katsenovich, F.R. Miralles-Wilhelm, Evaluation of nanoscale zerovalent iron
271 particles for trichloroethene degradation in clayey soils, Sci. Tot. Environ. 407 (2009),
272 4986–4993.
273 [28] S. Choe, S.-H. Lee, Y.-Y. Chang, K.-Y. Hwang, J. Khim, Rapid reductive destruction of
274 hazardous organic compounds by nanoscale Fe^0, Chemosphere 42 (2001), 367–72.
275 [29] H.-L. Lien, W.-x. Zhang, Nanoscale iron particles for complete reduction of chlorinated
276 ethenes, Colloid Surf. A191 (2001), 97–105.
277 [30] J.T. Nurmi, P.G. Tratnyek, V. Sarathy, D.R. Baer, J.E. Amonette, K. Pecher, C. Wang,
278 J.C. Linehan, D.W. Matson, R.L. Penn, M.D. Driessen, Characterization and properties
279 of metallic iron nanoparticles: spectroscopy, electrochemistry, and kinetics, Environ.
280 Sci. Technol. 39 (2005), 1221–1230.

[31] J. Nawrocki, U. Raczyk-Stanisawiak, J. Swietlik, A. Olejnik, M.J. Sroka, Corrosion in a distribution system. Steady water and its composition, Water Res. 44 (2010), 1863–1872.

[32] M. Stratmann, J. Müller, The mechanism of the oxygen reduction on rust-covered metal substrates. Corros. Sci. 36 (1994), 327-359.

[33] R.W. Gillham, Discussion of Papers/Discussion of nano-scale iron for dehalogenation. by Evan K. Nyer and David B. Vance (2001), Ground Water Monitoring & Remediation v. 21, no. 2, pages 41–54. Ground Water Monit. Remed 23 (2003), 6–8.

[34] C. Noubactep, A. Schöner, G. Meinrath, Mechanism of uranium (VI) fixation by elemental iron, J. Hazard. Mater. 132 (2006), 202–212

Table 1: Overview on the differential reactivity of microscale (d_1 = 50 μm) and nanoscale (d_2 = 50 nm) metallic iron as reflected by the difference of the number of Fe atom at the surface of individual particles. N is the total number of particles in 250 mg of the material. N' is the number of Fe atoms per particle (sphere). N'' is the number of Fe atoms at the surface of the individual spheres. N^1 = N * N'' is the total number of Fe^0 which is exposed to the aqueous solution and could be oxidized to Fe^{II} in the first stage assuming uniform corrosion (first stage of monolayer dissolution).

Material	**N**	**N'**	**N''**	**N^1**	**N^1**
	(-)	(-)	(-)	(atoms)	(moles)
Micro-Fe^0	489510	$5.56*10^{15}$	$1.91*10^{11}$	$9.36*10^{16}$	$1.55*10^{-7}$
Nano-Fe^0	$4.90*10^{14}$	$5.56*10^{6}$	$1.91*10^{5}$	$9.36*10^{19}$	$1.55*10^{-4}$

Table 2: Comparison of the experimental conditions of Katsenovich and Miralles-Wilhelm [27] and three therein referenced articles on remediation with nano-Fe^0. SSA is the specific surface area. The large variability of used experimental conditions evidences the difficulty of comparing achieved results. In particular, the molar ratio Fe^0/contaminant varies from 26 to 1160.

Contaminant (X)	**[X]** (mg/L)	**Material**	**Fe^0 size**	**SSA** (m^2/g)	**[Fe^0]** (mg)	**V** (L)	**[Fe^0]/[X]** (-)	**Ref.**
Trichloroethene	9.0	Fe^0	120 nm	6	50	150	86	[27]
	9.0	Fe^0	120 nm	6	125	150	215	
	9.0	Fe^0	120 nm	6	200	150	344	
Trichloroethylene	10.0	Fe^0	1 - 200 nm	31.4	625	125	1170	[28]
Chloroform	10.0	Fe^0	1 - 200 nm	31.4	625	125	1065	
Nitrobenzene	10.0	Fe^0	1 - 200 nm	31.4	625	125	1100	
Nitrotoluene	10.0	Fe^0	1 - 200 nm	31.4	625	125	1225	
Dinitrobenzene	10.0	Fe^0	1 - 200 nm	31.4	625	125	1513	
Dinitrotoluene	10.0	Pd^0/Fe^0	1 - 200 nm	31.4	625	125	1653	
Tetrachloroethene	20.0	Pd^0/Fe^0	10-100 nm	35	250	50	740	[29]
Trichloroethene	20.0	Pd^0/Fe^0	10-100 nm	35	250	50	587	
1,1-dichloroethene	20.0	Pd^0/Fe^0	10-100 nm	35	250	50	433	
Cis-1,2-dichloroethene	20.0	Pd^0/Fe^0	10-100 nm	35	250	50	433	
Trans-1,2-dichloroethene	20.0	Pd^0/Fe^0	10-100 nm	35	250	50	433	
Vinyl chloride	20.0	Pd^0/Fe^0	10-100 nm	35	250	50	279	
Carbon tetrachloride	0.6	Fe^0	70 nm	29	150	120	5580	[30]
Carbon tetrachloride	0.6	Fe^0	10-100 nm	33.5	300	120	11161	
Carbon tetrachloride	132.6	Fe^0	70 nm	29	150	120	26	
Carbon tetrachloride	132.6	Fe^0	10-100 nm	33.5	300	120	52	

Figure 1

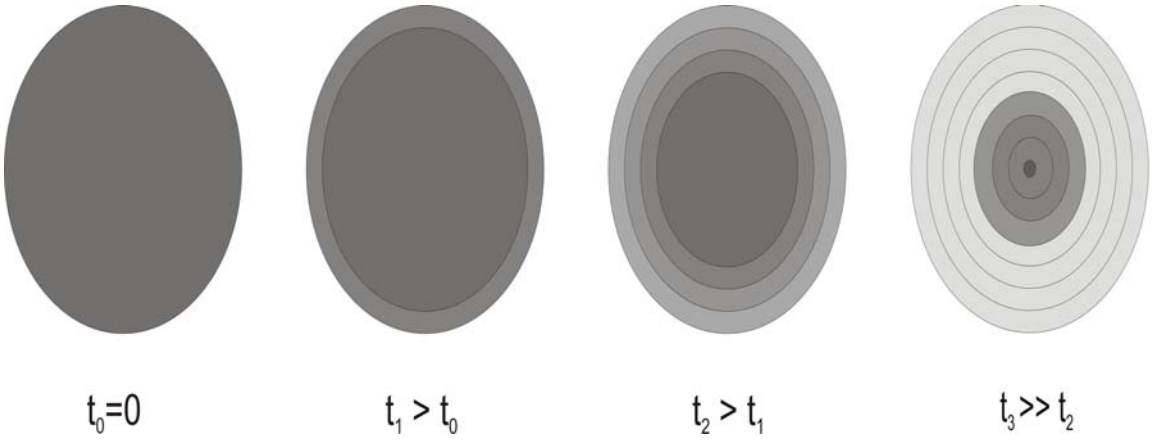

315 **Figure 2**

316

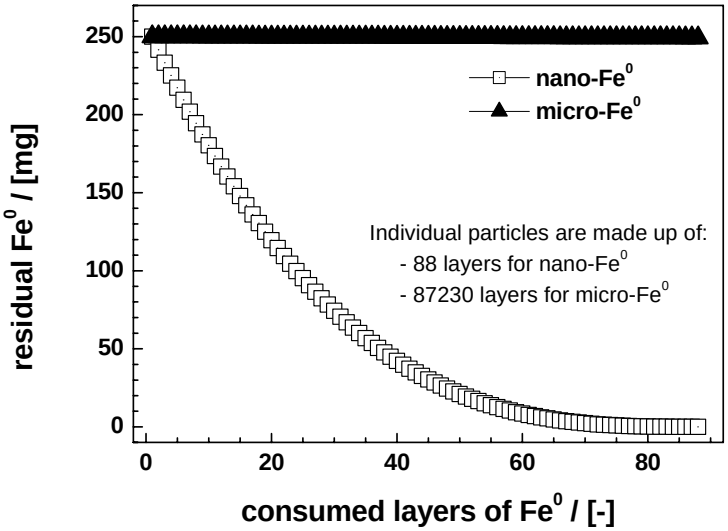

317

318

319

Figure captions

Figure 1: Time dependence consumption of Fe^0 from a spherical material assuming uniform corrosion. Initial concentric layers of Fe^0 atoms are progressively transformed to concentric layers of iron hydroxides which are further transformed to iron oxides.

Figure 2: Residual mass of metallic iron (Fe^0) as function of consumed layers from individual Fe^0 particles. It is evident that nano-Fe^0 is depleted as only 0.30 % of micro-Fe^0 is consumed. Uniform corrosion is assumed and material is supposed to be ideal concentric layers of Fe^0. Accordingly a nanoscale particle is made up of 88 layers of Fe^0.